NJC

PAPER

View Article Online
View Journal | View Issue

Cite this: *New J. Chem.*, 2015, 39, 909

The spontaneous room temperature reduction of $HAuCl_4$ in ethylene glycol in the presence of ZnO: a simple strategy to obtain stable Au/ZnO nanostructures exhibiting strong surface plasmon resonance and efficient electron storage properties†

Matías E. Aguirre,[a] Gonzalo Perelstein,[a] Armin Feldhoff,[b] Adriana Condó,[c] Alfredo J. Tolley[c] and María A. Grela*[a]

Received (in Porto Alegre, Brazil) 26th September 2014,
Accepted 10th November 2014

DOI: 10.1039/c4nj01663g

www.rsc.org/njc

The room temperature spontaneous reduction of $HAuCl_4$ in ethylene glycol in the presence of pre-formed ZnO nanoparticles is investigated by UV-vis spectroscopy. Analysis by HRTEM demonstrated that the synthesized nanostructures consist of small ZnO nanoparticles (5.0 nm) in contact with bigger (15 nm) spherical Au nanoparticles. The electronic communication between Au and ZnO blocks is confirmed by UV excitation of the colloid. These experiments indicate that ZnO nanoparticles efficiently transfer the electrons to Au nanoparticles in contact, inducing a 15 nm blue shift in the plasmon band. Titration experiments using the methylviologen couple ($MV^{2+}/MV^{\bullet+}$) are presented and analyzed to quantify the enhancement in the electron storage capability in the new nanostructure and the negative shift in the Fermi level caused by the Au loading in ZnO.

Introduction

The development of synthetic methods to produce metal nanoparticles and composite metal–semiconductor nanostructures is an active area of research.[1–4] The interest for these materials is motivated in their broad range of applications that include catalysis,[5] optoelectronics,[6,7] information processing, sensing[8] and biological applications.[9,10] Recent advances in the preparation and assembly of metal nanostructures have opened up new opportunities for precise control of their interaction with light through the modulation of their plasmon band.[11]

Noble metal nanoparticles can be synthesized by many chemical methods,[12] the most popular being the reduction of the precursor salts by citrate, introduced by Turkevich in 1951,[13] the synthesis of Brust involving a two phase process using sodium borohydride as a reductant[14] or the polyol process developed by Fiévet and co-workers.[15] The primary reaction of the latter process involves the reduction of the metal precursor by the polyol at elevated temperatures in the presence of a stabilizer, usually poly(vinylpyrrolidone), PVP.[16] The temperature dependent reducing power of the polyols[17] together with the known ability of PVP as a shape directing agent[18] has been exploited to control the nucleation and growth processes *i.e.*, to modulate the size and morphology of the metal nanoparticles by changing the reaction temperature and the concentration of the stabilizer.[19,20]

The development of plasmon bands in the visible region is of particular interest since their excitation can trigger chemical transformations of species in the vicinity of the nanostructure by the enhanced generation of excited states, thermal activation or hole-transfer. The latter process is supposed to be favoured in metal–semiconductor nanostructures, where the injection of the plasmon photoinduced electrons into the CB of the semiconductor may assist charge separation.[21] However, to make this mechanism feasible, metal and semiconductor domains should be in direct contact avoiding the presence of stabilizers, insulating layers or molecular linkers since electron injection competes with the rapid electron scattering process.[22]

Here we report on a simple method for obtaining Au/ZnO nanocomposites in ethylene glycol at room temperature which does not require the addition of stabilizers or other reducing agents. Interestingly the synthesized material displays a sharp plasmonic band peaking at 535 nm and is stable for months. HRTEM studies indicate that the Au/ZnO nanostructures are formed by small ZnO nanoparticles (5 ± 0.8 nm) partially

[a] *Departamento de Química, Universidad Nacional de Mar del Plata, Funes 3350, B7602AYL Mar del Plata, Argentina. E-mail: magrela@mdp.edu.ar*
[b] *Institut für Physikalische Chemie und Elektrochemie, Leibniz Universität Hannover, Callinstraße 3a, D-30167 Hannover, Germany*
[c] *Centro Atómico Bariloche, R8400AGQ San Carlos de Bariloche, Río Negro, Argentina*

† Electronic supplementary information (ESI) available. See DOI: 10.1039/c4nj01663g

covered by relatively bigger (15 ± 5 nm) spherical Au nanoparticles. The electronic contact between the building blocks is assessed by a blue shift of 15 nm obtained by UV excitation of Au/ZnO. Titration experiments using the methylviologen couple ($MV^{2+}/MV^{\bullet+}$) are presented and analyzed to quantify the enhancement in the electron storage capability in the new nanostructure and the negative shift in the Fermi level caused by the Au loading in ZnO.

Experimental section

Materials

Methylviologen dichloride hydrate, 98%, (Aldrich), hydrogen tetrachloroaurate trihydrate, 99.9%, (Aldrich), zinc acetate dihydrate (Fluka), sodium hydroxide (Merck), tetramethylammonium hydroxide (Sigma) were of the highest available purity and used as received. Ethylene glycol (Biopack), 1-octanol (extra pure grade, Merck), ethyl acetate (Sintorgan), heptane (Sintorgan) and dimethylsulfoxide (chromatographic grade, Sintorgan) were used without further purification.

Methods

Preparation of ZnO nanoparticles. Colloidal ZnO nanocrystals were synthesized by alkaline hydrolysis/condensation reactions induced by the drop wise addition of tetramethylammonium hydroxide to a solution of zinc acetate in dimethylsulfoxide, following previous published procedures.[23] Briefly, 6.25 mL of a 550 mM solution of tetramethylammonium hydroxide in ethanol was slowly added to 20 mL of a 0.1 M solution of zinc acetate in dimethyl sulfoxide. The reaction was stopped by precipitation of the nanocrystals with ethyl acetate, and repeatedly purified from the solvents and excess reagents by two cycles of heptane-induced precipitation, and resuspension in ethanol.

Preparation of Au/ZnO materials. About 350 mg of ZnO nanoparticles were dispersed in 10 mL of ethylene glycol, the suspension was magnetically stirred 20 min, then sonicated 10 min, and finally subjected to three 5 min centrifugation cycles at 9770*g* in a Sorvall RC5C ultracentrifuge. After each centrifugation cycle the supernatant suspension was carefully transferred to a clean tube. In a typical procedure 25 mL of a 1.25 mM $HAuCl_4$ solution in ethylene glycol was mixed with 25 mL of a ZnO suspension Absorbance (348 nm) = 14.0. The mixture was bubbled with air at room temperature.

Glassware was cleaned with sulfochromic acid, washed with a non ionic detergent and wiped away with ultrapure water.

Characterization. Optical absorption spectra of the Au/ZnO nanocomposites were recorded on an Agilent 8453 diode array spectrophotometer.

The crystalline properties of ZnO and Au/ZnO nanostructures were examined *via* powder X-ray diffraction (XRD). The analysis was carried out on a X'Pert PRO (PANalytical) powder X-ray diffractometer, with CuKα (1.54 Å) as the incident radiation and operated at an accelerating voltage of 40 kV with a current intensity of 40 mA. The samples for XRD analysis were prepared by precipitation of the nanocomposites dispersed in ethylene glycol with 1-octanol. The solid was repeatedly washed with small amounts of ethanol, and finally dried under a nitrogen stream and then heated at 120 °C.

ZnO and Au/ZnO nanocomposites were also investigated by transmission electron microscopy (HRTEM) using a Philips CM200 LaB_6 microscope and a Tecnai F20 field-emission instrument, equipped with EDAX energy-dispersive X-ray spectrometers (EDXS). A *ca.* 10 μL drop of colloidal suspension was put on a copper-supported formvar–carbon foil and dried under a red light lamp.

Results and discussion

Formation of Au/ZnO nanostructures

Fig. 1 shows the UV-vis absorption spectra of ZnO nanoparticles dispersed in ethylene glycol. The onset of absorption of the as-synthesized nanoparticles was found at energies higher than that of the ZnO bulk bandgap, demonstrating that they are in the quantum confinement regime. An average diameter $\langle d \rangle$ = 5.0 nm was evaluated from the UV-visible absorption spectra using available models, based on the effective mass approximation.[24,25] For details see S1 (ESI†). The inset shows the XRD pattern of powders which confirms the formation of hexagonal wurzite nanocrystal particles, JCPDS card #36-1451.[26]

Fig. 2 shows the evolution of the UV-vis spectra of a 0.16 mM $HAuCl_4$ solution in a 2 mM ZnO sol maintained at constant temperature (298 K) and stirred by air-bubbling.

Absorption measurements were performed in a quartz cuvette (l = 0.5 cm). For clarity, the data are presented in two panels, as the absorbance in the UV region at $\lambda < 370$ nm decreases in the first ten minutes and then increases together with the appearance of a visible band. The solid curve of the upper panel shows the theoretical initial absorbance (denoted as $t = 0^*$ minutes) obtained as simple sum of the contributions of the individual species, and the rest of the curves show the following absorbance spectra obtained upon mixing the solutions.

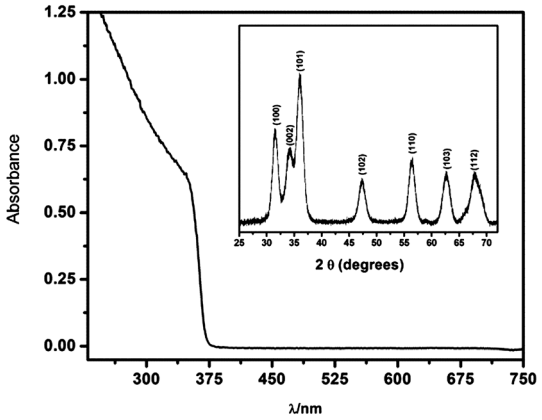

Fig. 1 UV-vis spectra of ZnO nanoparticles dispersed in ethylene glycol. Inset XRD pattern of powders obtained by ultracentrifugation of the as-prepared ZnO sol, the peaks corresponding to the reflection from the crystal planes of ZnO are indicated between brackets.

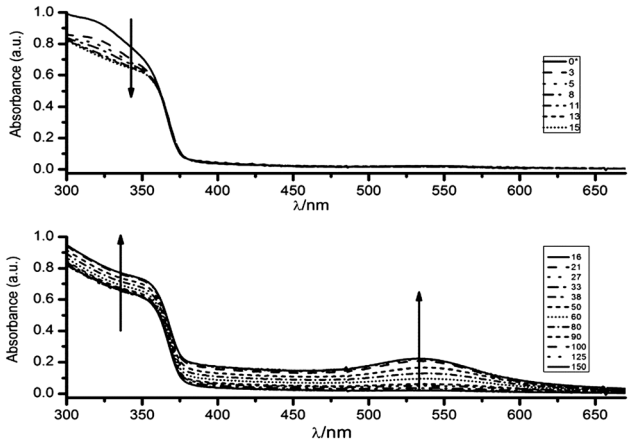

Fig. 2 Time dependence of the UV-vis spectrum of a solution 0.16 mM $HAuCl_4$ and 2 mM ZnO in ethylene glycol. Time is denoted in minutes. The upper panel shows the evolution of the spectrum in the first 15 minutes after the mixing process, and shows that the absorbance of Au(III) species decays without forming Au(0), the lower panel indicates the raising of the band in the visible and UV region, for times between 15 and 150 minutes, due to the formation of Au nanoparticles, see the text.

The high viscosity of ethylene glycol somehow prevents a good measure of the initial value. However, the first determination, obtained after 3 minutes of reaction, indicates a rapid depletion of the band attributable to the Au(III) species in pure ethylene glycol. This observation is followed by a slower decay of the absorbance range between 290 and 350 nm.

As shown in the lower panel of Fig. 2, a visible band centred at 535 nm, appears after the UV-vis spectrum in the region below 350 nm has recovered the absorption characteristics of ZnO. This feature indicates the formation of spherical Au nanoparticles with a moderate size distribution.

It should be stressed that the presence of ZnO was found to be necessary for the development of the plasmon band, which is indicative of the complete reduction of Au(III) to Au(0). In contrast, the evolution of the UV-vis spectra of a 0.11 mM $HAuCl_4$ solution in pure ethylene glycol shows that the ligand-to-metal charge transfer (LMCT) band of the $AuCl_4^-$ at 322 nm slowly decreases, with an apparent half-life time, $\tau \sim 1200$ minutes (see S3, ESI†). It is worthwhile to notice that in the absence of ZnO the reduction ends in Au(I) species, as the UV-vis spectra remain invariable once the absorption at 322 nm bleaches. The formation of small ($d < 5$ nm) subplasmonic nanoparticles was discarded by determining that there were no fluorescent signals upon excitation at λ = 270–300 nm which are typically observed for gold nanoclusters.[27] The above results clearly indicate that in homogeneous systems it is necessary to enhance the moderate reducing power of ethylene glycol by photochemical or thermal activation[12] in order to obtain Au nanoparticles, and lends additional support to the fact that Au(0) is formed on ZnO nanoparticles. On the other hand, the thermal and photochemical[28] production of Au nanoparticles in ethylene glycol revealed that Au nanoparticles readily agglomerate and precipitate unless a suitable stabilizer is added during the synthesis.[15,16] By these evidences we can safely discard the presence of free Au nanoparticles as products of our synthetic approach.

Au/ZnO nanostructures were characterized by XRD and HRTEM. Additionally, TEM was combined with energy dispersive X-ray spectroscopy (EDXS) and used during the measurements also as a scanning transmission electron microscope (STEM) to obtain high-angle annular dark-field (HAADF) micrographs and the phase distribution. This last information is shown in Fig. S2, in the ESI.†

The XRD pattern of the Au/ZnO nanostructure, Fig. 3, shows in addition to the peaks corresponding to the reflection from the crystal planes of ZnO observed in the inset of Fig. 1, those characteristic of Au nanoparticles, JCPDS card No. 04-0784. HRTEM analysis shown in Fig. 4 apparently indicates that ZnO surrounds Au nanoparticles partially, but they do not form a closed shell. Notice that the formation of a perfect shell, covering Au nanoparticles, would be detrimental for our purposes, *i.e.*, for their utilization in plasmonic photocatalysis. We have already performed additional experiments, results not shown, involving the visible excitation of the synthesized nanostructure to demonstrate that under these conditions, an electron from Au can be transferred to the semiconductor and that the hole left in the metal can be replenished by a donor added to a dispersion of the nanostructures in ethylene glycol.

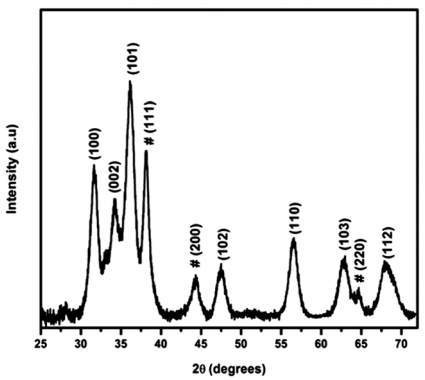

Fig. 3 XRD pattern of the powder Au ZnO nanostructures. The peaks corresponding to the reflection from the crystal planes of ZnO (JCPDS card No. 036-1451) and Au (#, JCPDS card No. 04-0784) are indicated between brackets.

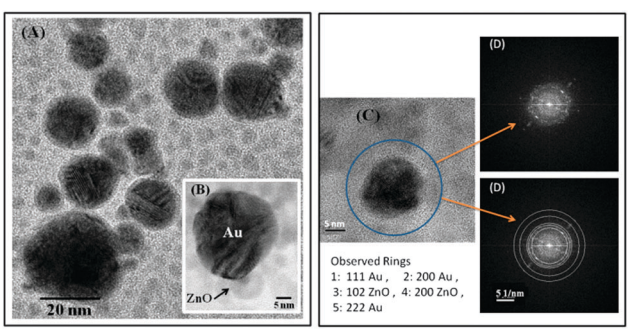

Fig. 4 (A) HRTEM image of the nanostructures obtained under magnification. In the expanded view, inset (B), the contact between ZnO and Au is clearly discernible. Panel (D) shows the periodicity of image C by the FFT (Fast Fourier Transform) spectra calculated with the Digital Micrograph software. The same rings were clearly distinguished in the electron diffraction pattern of the Au/ZnO nanostructures.

Mechanism of formation of Au/ZnO nanostructures

The adsorption of gold chloride and gold hydroxyl chlorides $[Au(OH)_{4-x}Cl_x]^-$ complexes on titanium dioxide and other oxides has been considered in the literature, in connection with the loading of Au nanoparticles over the semiconductors by deposition–precipitation methods[29] or photoreduction.[30,31] Due to its amphoteric character, semiconductor metal oxides can attract both positive and negative ions depending on whether the pH of the media lies above or below the zero point charge, respectively.[32] Besides the pure electrostatic interaction, the high fraction of undercoordinated atoms at the surface of the nanoparticles enhances their reactivity toward binding. In this context, it has been proposed that the interaction of gold hydroxy chlorides with aqueous titanium dioxide[30] or alumina[32] involves a reaction with surface M–OH groups available at the oxide–water interface to form an inner-sphere complex

$$MOH + [Au(OH)_{4-x}Cl_x]^- = MAu(OH)_{3-x}Cl_{x-1} + H_2O + Cl^- \quad (1)$$

In the above equation M stands for the metal (M = Ti, Al), and the terminal coordinating OH group is the result of the dissociative water chemisorption.

A detailed description of the adsorption processes of inorganic and organic species is not simple, because it requires the definition of a particular crystal face at which the chemisorption takes place.[33] Although there is still a considerable gap between the theoretical pictures and a realistic description of the processes taking place at the metal oxide interface, computational studies had shed some light on the specific ways that water[34] and other ligands bearing definite anchor groups (as 1,2 OH moieties) interact with the ZnO surface.[35]

Based on these studies, to rationalize the reduction of Au(III) species on ZnO we assume that before the addition of $AuCl_4^-$, the semiconductor surface is covered by water and ethylene glycol molecules. The capping action of ethylene glycol towards ZnO nanoparticles has been assessed by FTIR spectroscopy[36] and exploited to control the size and agglomeration state of ZnO nanoparticles.[37] Upon addition of Au(III) species, the electrostatic attraction between gold chloride complexes (or chlorohydroxy complexes formed by the small amount water present in the solvent) and the positive charged ZnO surface brings these partners in close contact, and favours the chemical adsorption of the gold precursors on the defect sites of ZnO by substitution of one of the chloride ligands by a hydroxyl group on the surface of ZnO. The reaction between Au and ethylene adsorbed on neighbouring positions of the surface probably leads to the oxidation of the carbon atom associated with the OH group to aldehyde with the concomitant reduction of Au(III) to Au(I), which then is further reduced to Au(0).

It is interesting to notice that the plasmon band does not appear until the absorbance because Au(III) species has disappeared completely. This fact may be accounted considering the comproportionation reaction of nascent gold atoms with Au(III) species, as recently proposed by Belloni and co-workers:[38]

$$Au(III) + Au(0) \rightarrow Au(II) + Au(I) \quad (2)$$

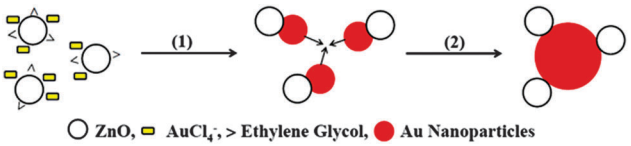

Scheme 1 Mechanism of formation of the plasmonic nanostructures. The adsorption of Au(III) species on ZnO facilitates its reduction to Au(0), (1). Process (2) indicates the agglomeration of the nascent Au nanoparticles to give the final nanostructure.

Once all Au(III) has been removed from the system, the agglomeration of Au(0) species as shown in Scheme 1 produces the plasmon band, and in turn explains the observed morphology of the nanostructures.

Assessing the contact between Au and ZnO blocks

It has been shown that UV-irradiation of a sol of ZnO nanoparticles in the absence of suitable electron scavengers leads to a blue shift in the absorption spectra. This phenomenon, referred to in the literature as the Moss–Burstein effect, can be used to ascertain the accumulation of conduction band electrons in semiconductor nanoparticles.[39]

Electrochemical and photochemical experiments indicate that charged ZnO nanoparticles can transfer the electrons to Au nanoparticles in contact, increasing the number of accumulated charge carriers within the system. The storage of multiple electrons during the UV irradiation of Au/ZnO nanostructures drives the overall Fermi level of the system to more negative potentials.[40–42]

We have monitored the UV-vis spectra of pure ZnO and Au/ZnO nanostructures to investigate the effect of the metal on charge storage during the anaerobic irradiation at 303 ± 10 nm. In both cases we found that the excitonic band of ZnO progressively shifts to the blue until it reaches a steady state. However the irradiation of the Au/ZnO nanostructures additionally results in a shift of the plasmon band from 535 to 520 nm (see Fig. 5).

This change is indicative of the increased electron density in the metal, and can be taken as strong evidence that the

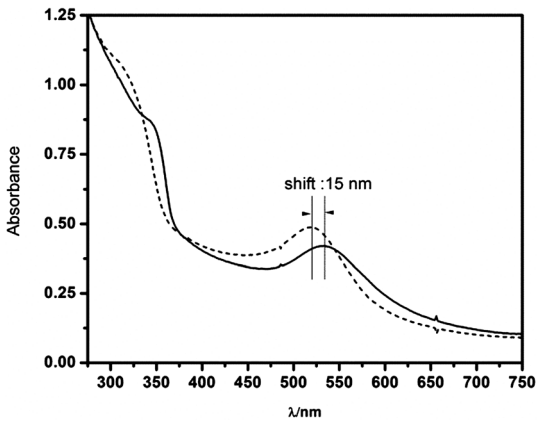

Fig. 5 UV-vis spectra of the Au/ZnO nanostructures obtained before (solid line) and after (dashed line) anaerobic, 303 ± 10 nm irradiation.

junction between ZnO and Au nanoparticles in the nanostructure allows the transfer of electrons across the interface.[43] It should be stressed that the original spectra can be completely recovered by admitting air into the cell, indicating that Au nanostructures are not affected by the UV irradiation.

On the other hand, the number of electrons stored – after reaching the steady state under anaerobic 303 nm irradiation – was evaluated by the production of the methyl viologen cation radical MV^{+} from MV^{2+}, according to reaction (3):

$$MV^{2+} + e^{-} \rightarrow MV^{+\bullet} \qquad (3)$$

We found that 0.0051 and 0.0173 μmoles of MV^{2+} are used to titrate the electrons stored in ZnO and Au/ZnO nanostructures, respectively. As reported elsewhere, these experiments allow the determination of the apparent Fermi level of the electrons after equilibration with the $MV^{2+}/MV^{+\bullet}$ couple using eqn (4):

$$E_F = E^0(MV^{2+}/MV^{+\bullet}) - 0.059 \log \frac{[MV^{+}]}{[MV^{2+}]} \qquad (4)$$

where $E^0(MV^{2+}/MV^{+\bullet}) = -0.44$ V is the standard reduction potential of the $MV^{2+}/MV^{\bullet+}$ redox couple. Our results indicate that the higher accumulation of electrons in Au/ZnO nanostructures results in the negative direction producing a 32 mV shift of the apparent Fermi level upon equilibration from −0.299 to −0.331 V (see ESI† for details).

Using electron paramagnetic resonance, we have recently proved that the synthesized nanostructures can also be used in the plasmon photoinduced electron transfer process in the metal → semiconductor direction under selective visible irradiation, and that the hole in the metal can be replenished by a convenient donor added to the dispersion of the nanostructures in ethylene glycol.[44] These results indicate that by modulating the excitation wavelength the electron flow direction can be switched in both directions. We are actively investigating these issues.

Conclusions

In summary we have shown that $HAuCl_4$ can be spontaneously reduced in ethylene glycol in the presence of pre-formed ZnO nanoparticles at room temperature leading to Au/ZnO nanostructures with a sharp plasmonic band, and not requiring the presence of additional stabilizers. The electronic contact between ZnO and Au and the enhancement in electron accumulation caused by Au loading were assessed by UV irradiation in the absence of acceptors followed by MV^{2+} titration experiments in the dark.

Acknowledgements

The authors thank Dr M. Desimone (Intema, CONICET) for technical assistance in the XRD analysis. This work was financially supported by the University of Mar del Plata and the National Research Council of Argentina (CONICET), project PIP 416. MEA thanks CONICET for a doctoral fellowship.

References

1 N. Zhang, S. Liu and Y.-J. Xu, *Nanoscale*, 2012, **4**, 2227–2238.
2 S. Linic, P. Christopher, H. Xin and A. Marimuthu, *Acc. Chem. Res.*, 2013, **46**, 1890–1899.
3 X. Zhou, G. Liu, J. Yu and W. Fan, *J. Mater. Chem.*, 2012, **22**, 21337–21354.
4 C. Mondal, J. Pal, M. Ganguly, A. K. Sinha, J. Jana and T. Pal, *New J. Chem.*, 2014, **38**, 2999–3005.
5 M. Haruta, *CATTECH*, 2002, **6**, 102–115.
6 X. Li, G. Chen, L. Yang, Z. Jin and J. Liu, *Adv. Funct. Mater.*, 2010, **20**, 2815–2824.
7 J. Qi, X. Dang, P. T. Hammond and A. M. Belcher, *ACS Nano*, 2011, **5**, 7108–7116.
8 F. Boccuzzi, A. Chiorino, S. Tsubota and M. Haruta, *Sens. Actuators, B*, 1995, **25**, 540–543.
9 W.-Q. Zhang, Y. Lu, T.-K. Zhang, W. Xu, M. Zhang and S.-H. Yu, *J. Phys. Chem. C*, 2008, **112**, 19872–19877.
10 X. Wang, X. Kong, Y. Yu and H. Zhang, *J. Phys. Chem. C*, 2007, **111**, 3836–3841.
11 M. Rycenga, C. M. Cobley, J. Zeng, W. Li, C. H. Moran, Q. Zhang, D. Qin and Y. Xia, *Chem. Rev.*, 2011, **111**, 3669–3712.
12 D. V. Goia and E. Matijević, *New J. Chem.*, 1998, **22**, 1203–1215.
13 J. Turkevich, P. C. Stevenson and J. Hillier, *Discuss. Faraday Soc.*, 1951, **11**, 55–75.
14 M. Brust, M. Walker, D. Bethell, D. J. Schiffrin and R. Whyman, *J. Chem. Soc., Chem. Commun.*, 1994, **7**, 801–802.
15 F. Fiévet, J. P. Lagier, B. Blin, B. Beaudoin and M. Figlarz, *Solid State Ionics*, 1989, **32**, 198–205.
16 P. Y. Silvert and K. Tekaia-Elhsissen, *Solid State Ionics*, 1995, **82**, 53–60.
17 A. R. Tao, S. Habas and P. Yang, *Small*, 2008, **4**, 310–325.
18 I. Pastoriza-Santos and L. M. Liz-Marzan, *Adv. Funct. Mater.*, 2009, **19**, 679–688.
19 F. Kim, S. Connor, H. Song, T. Kuykendall and P. Yang, *Angew. Chem., Int. Ed.*, 2004, **116**, 3673–3677.
20 Y. Sun and Y. Xia, *Science*, 2002, **298**, 2176–2179.
21 S. Linic, P. Christopher and D. B. Ingram, *Nat. Mater.*, 2011, **10**, 911–921.
22 J. C. Scaiano and K. Stamplecoskie, *J. Phys. Chem. Lett.*, 2013, **4**, 1177–1187.
23 D. A. Schwartz, N. S. Norberg, Q. P. Nguyen, J. M. Parker and D. R. Gamelin, *J. Am. Chem. Soc.*, 2003, **125**, 13205–13218.
24 L. Brus, *J. Phys. Chem.*, 1986, **90**, 2555–2560.
25 N. S. Pesika, K. J. Stebe and P. C. Searson, *J. Phys. Chem. B*, 2003, **107**, 10412–10415.
26 American Society for Testing and Material, *American Society for Testing and Material, Powder Diffraction Files*, Joint Committee on Powder Diffraction Standards, Swarthmore, PA, 1999, pp. 3–888.
27 X. Liu, C. Li, J. Xu, J. Lv, M. Zhu, Y. Guo, S. Cui, H. Liu, S. Wang and Y. Li, *J. Phys. Chem. C*, 2008, **112**, 10778–10783.
28 S. Eustis, H. Y. Hsu and M. A. El-Sayed, *J. Phys. Chem. B*, 2005, **109**, 4811–4815.
29 R. Zanella, S. Giorgio, C. R. Henry and C. Louis, *J. Phys. Chem. B*, 2002, **106**, 7634–7642.

30 T. Soejima, H. Tada, T. Kawahara and S. Ito, *Langmuir*, 2002, **18**, 4191–4194.
31 C.-Y. Wang, C.-Y. Liu, X. Zheng, J. Chen and T. Shen, *Colloids Surf., A*, 1998, **131**, 271–280.
32 S. Ivanova, C. Petit and V. Pitchon, *Appl. Catal., A*, 2004, **267**, 191–201.
33 W. Macyk, K. Szacilowski, G. Stochel, M. Buchalska, J. Kuncewicz and P. Labuz, *Coord. Chem. Rev.*, 2010, **254**, 2687–2701.
34 D. Raymand, A. C. T. van Duin, W. A. Goddard, K. Hermansson and D. Spangberg, *J. Phys. Chem. C*, 2011, **115**, 8573–8579.
35 A. Calzolari, A. Ruini and A. Catellani, *J. Am. Chem. Soc.*, 2011, **133**, 5893–5899.
36 R. S. Ningthoujam, N. S. Gajbhiye, A. Ahmed, S. S. Umre and S. J. Sharma, *J. Nanosci. Nanotechnol.*, 2008, **8**, 3059–3062.
37 T. Ghoshal, S. Kar and S. Chaudhuri, *Cryst. Growth Des.*, 2006, **7**, 136–141.
38 G. R. Dey, A. K. El Omar, J. A. Jacob, M. Mostafavi and J. Belloni, *J. Phys. Chem. A*, 2011, **115**, 383–391.
39 (*a*) Y. Di Iorio, M. E. Aguirre, M. A. Brusa and M. A. Grela, *J. Phys. Chem. C*, 2012, **116**, 9646–9652; (*b*) I. K. Levy, M. A. Brusa, M. E. Aguirre, G. Custo, E. San Roman, M. I. Litter and M. A. Grela, *Phys. Chem. Chem. Phys.*, 2013, **15**, 10335–10338.
40 A. Wood, M. Giersig and P. Mulvaney, *J. Phys. Chem. B*, 2001, **105**, 8810–8815.
41 V. Subramanian, E. E. Wolf and P. V. Kamat, *J. Phys. Chem. B*, 2003, **107**, 7479–7485.
42 M. Tsuji, N. Miyamae, M. Hashimoto, M. Nishio, S. Hikino, N. Ishigami and I. Tanaka, *Colloids Surf., A*, 2007, **302**, 587–598.
43 A. Takai and P. V. Kamat, *ACS Nano*, 2011, **5**, 7369–7376.
44 M. Aguirre, G. M. Perelstein and M. A. Grela, *Abstract presented in the Physical and Inorganic Chemistry Argentinean Meeting*, AAIFQ Association, Rosario, Argentine, 2013, to be submitted for publication.

